

Rabex-5 Is a Rab22 Effector and Mediates a Rab22-Rab5 Signaling Cascade in Endocytosis

Huaiping Zhu, Zhimin Liang, and Guangpu Li

Department of Biochemistry and Molecular Biology, University of Oklahoma Health Sciences Center, Oklahoma City, OK 73104

Submitted June 8, 2009; Revised September 1, 2009; Accepted September 10, 2009
Monitoring Editor: Adam Linstedt

Rabex-5 targets to early endosomes and functions as a guanine nucleotide exchange factor for Rab5. Membrane targeting is critical for Rabex-5 to activate Rab5 on early endosomes in the cell. Here, we report the identification of Rab22 as a binding site on early endosomes for direct recruitment of Rabex-5 and activation of Rab5, establishing a Rab22-Rab5 signaling relay to promote early endosome fusion. Rab22 in guanosine 5'-O-(3-thio)triphosphate-loaded form, but not guanosine diphosphate-loaded form, binds to the early endosomal targeting domain (residues 81-230) of Rabex-5 in pull-down assays. Rabex-5 targets to Rab22-containing early endosomes, and Rab22 knockdown by short hairpin RNA abrogates the membrane targeting of Rabex-5 in the cell. In addition, coexpression of Rab22 and Rab5 shows synergistic enlargement of early endosomes, and this synergy is dependent on Rabex-5, providing further support for the collaboration of the two Rab GTPases in regulation of endosome dynamics. This novel Rab22-Rabex-5-Rab5 cascade is functionally important for the endocytosis and degradation of epidermal growth factor.

INTRODUCTION

Rab GTPases specifically target to distinct organelles and regulate intracellular membrane trafficking along and between endocytic and exocytic pathways (Stenmark and Olkkonen, 2001; Zerial and McBride, 2001; Grosshans *et al.*, 2006). Rab5, in particular, is localized to early endosomes and plasma membrane and regulates early membrane fusion in the cell (Bucci *et al.*, 1992; Li *et al.*, 1994; Stenmark *et al.*, 1994) as well as actin remodeling (Lanzetti *et al.*, 2004). Like other GTPases, Rab5 alternates between guanosine diphosphate (GDP)-bound and guanosine triphosphate (GTP)-bound conformations, and it is the GTP-bound form that is biologically active and interacts with effectors. One of such effectors is early endosomal antigen (EEA) 1, which functions as a tethering factor to promote early endosome fusion in endocytosis (Simonsen *et al.*, 1998; Christoforidis *et al.*, 1999).

Rab5 activation, i.e., Rab5-GDP to Rab5-GTP conversion, requires guanine nucleotide exchange factors (GEFs) that facilitate GDP dissociation and GTP loading. Rabex-5 is a well-documented Rab5 GEF (Horiuchi *et al.*, 1997; Lippe *et al.*, 2001). Rabex-5 knockout mice develop severe skin inflammation caused by enhanced immunoglobulin (Ig) E receptor-mediated degranulation and cytokine release from mast cells, which is due to loss of Rabex-5 GEF activity for Rab5 and reduced IgE receptor endocytosis/degradation

(Kalesnikoff *et al.*, 2007). Rabex-5 contains 492 amino acid residues, and the catalytic GEF domain resides in the middle region, encompassing residues 132-391 and consisting of a helical bundle (HB) domain and a Vps9 domain in tandem (Delprato *et al.*, 2004). Rabex-5 contains no transmembrane domain but can target to early endosomal membrane for Rab5 activation by two mechanisms. An indirect mechanism is mediated by the Rabaptin-5-binding domain immediately downstream of the GEF domain, which leads to the formation of Rabex-5/Rabaptin-5 complexes (Lippe *et al.*, 2001; Mattera *et al.*, 2006; Delprato and Lambright, 2007; Kalesnikoff *et al.*, 2007; Zhu *et al.*, 2007). Rabaptin-5 is a Rab5 effector that binds to Rab5-GTP on early endosomes (Stenmark *et al.*, 1995; Zhu *et al.*, 2004) and brings Rabex-5 to the proximity of more substrates (Rab5-GDP) on the target membrane, which may lead to further Rab5 activation in a positive feedback loop. In addition, a direct membrane targeting mechanism is mediated by the early endosomal targeting (EET) domain that is composed of a membrane-binding motif immediately upstream of the GEF domain and the following HB domain, thus overlapping with the GEF domain (Zhu *et al.*, 2007). The EET domain-mediated direct membrane targeting allows Rabex-5 to associate with early endosomes and activate Rab5 independent of Rabaptin-5, which may generate a relatively high basal level of Rab5-GTP on early endosomes to facilitate recruitment of Rabex-5/Rabaptin-5 complexes for further Rab5 activation and establishment of functional Rab5-GTP domains in endosome fusion. However, the nature of the EET domain binding site on early endosomes is yet to be determined. In addition, a recent study suggests that the N-terminal ubiquitin-binding regions also contribute to direct Rabex-5 targeting to early endosomes (Mattera and Bonifacino, 2008).

In the current study, we find that Rab22, in its GTP-bound form, serves as the early endosomal binding site for the EET domain of Rabex-5 and is responsible for direct Rabex-5 targeting to early endosomes. Rab22 is another Rab GTPase localized on early endosomes and is closely related to Rab5

This article was published online ahead of print in *MBC in Press* (<http://www.molbiolcell.org/cgi/doi/10.1091/mbc.E09-06-0453>) on September 16, 2009.

Address correspondence to: Guangpu Li (guangpu-li@ouhsc.edu).

Abbreviations used: BHK, baby hamster kidney; EET, early endosomal targeting; EGF, epidermal growth factor; FL, full length; GEF, guanine nucleotide exchange factor; GFP, green fluorescent protein; GST, glutathione transferase; HB, helical bundle; RFP, red fluorescent protein; WT, wild type.

with 52% sequence identity (Olkkonen *et al.*, 1993; Kauppi *et al.*, 2002). Inhibition of Rab22 function via small interfering RNA (siRNA) blocks recycling of endocytosed cargoes such as transferrin receptor and MHC-I (Weigert *et al.*, 2004; Magadan *et al.*, 2006). Overexpression of Rab22 in the cell leads to enlargement of early endosomes (Kauppi *et al.*, 2002), similar to the effect of Rab5. Rab22 is a member of the Rab5 subfamily that also includes Rab5, Rab21, and Rab31 (also called Rab22b) (Pereira-Leal and Seabra, 2000; Stenmark and Olkkonen, 2001). Rabex-5 is specific for Rab5 and Rab21, whereas its GEF activity toward Rab22 and other Rabs decreases dramatically by two orders of magnitude or more (Delprato *et al.*, 2004). Here, we find that in contrast to its interaction with GDP-bound form of Rab5, Rabex-5 binds to GTP-bound Rab22 and is thus an effector for Rab22. It is Rab22 that recruits Rabex-5 to early endosomes for Rab5 activation, establishing a Rab22-Rab5 signaling relay in regulation of early endosome fusion in the cell.

MATERIALS AND METHODS

Recombinant Protein Expression

Rabex-5, Rab22, and Rab5 are referred to cow Rabex-5, human Rab22a, and human Rab5a, with the NCBI accessions NM_174591, NM_020673, and NM_004162, respectively.

Mammalian Cell Cultures and Transfection

Baby hamster kidney (BHK)-21 cells were cultured as described previously (Zhu *et al.*, 2007). The Rabex-5-deficient NF73 cells, which were mouse embryo fibroblasts isolated from Rabex-5 knockout mice (Kalesnikoff *et al.*, 2007), were kindly provided by Dr. S. J. Galli's laboratory at Stanford University (Stanford, CA). NF73 and HeLa cells were grown in 35-mm culture dishes with 3 ml of DMEM containing 10% fetal bovine serum (Invitrogen, Carlsbad, CA). Cells were transfected with the plasmid constructs expressing various Rabex-5, Rab22, and Rab5 proteins as indicated via FuGENE HD-mediated procedure (Roche Applied Science, Indianapolis, IN) and incubated at 37°C in a tissue culture incubator with 5% CO₂. The expression vectors included pcDNA3 (Invitrogen), pBI (Clontech, Mountain View, CA), and pSIREN-RetroQ-DsRed-Express (Clontech). The pBI vector can express two cloned proteins simultaneously, whereas the pSIREN-RetroQ-DsRed-Express vector can express a cloned short hairpin RNA (shRNA) and dsRed simultaneously. Protein expression was confirmed by immunoblot analysis, and intracellular localization and endosomal morphology were determined by confocal fluorescence microscopy (see below).

Immunoblot Analysis

Cells were lysed in 1% SDS (200 μ l/35-mm dish), and the lysates were sheared to reduce the stickiness by passing through a 26-gauge needle five times with a 1-ml syringe, followed by SDS-polyacrylamide gel electrophoresis (PAGE) and immunoblot assays by using the enhanced chemiluminescence reagents (GE Healthcare, Chalfont St. Giles, Buckinghamshire, United Kingdom). The primary antibodies used in the immunoblot assays were anti-Myc and anti-actin monoclonal antibody (mAb) from Sigma-Aldrich (St. Louis, MO), anti-Rabex-5 mAb from BD Biosciences (San Jose, CA), and anti-Rab22 rabbit polyclonal antibody from Proteintech Group (Chicago, IL). The results were quantified by densitometry using Densitometer SI (GE Healthcare).

Confocal Fluorescence Microscopy

We used a Leica confocal laser scanning microscope with Ar-488 and Kr-568 laser excitation in the Flow and Image laboratory on campus. BHK-21, HeLa, and NF73 cells were grown on coverslips with or without transfection. The plasmids used for transfection included pBI and pcDNA3 constructs expressing various green fluorescent protein (GFP)-Rabex-5, red fluorescent protein (RFP)-Rab22, and GFP-Rab5 proteins, and the pSIREN-RetroQ-DsRed-Express constructs expressing Rab22 shRNAs as indicated. Cells were incubated at 37°C for 24 or 48 h as indicated and then processed for confocal fluorescence microscopy to determine the morphology of endogenous or GFP-Rabex-5-, RFP-Rab22-, and GFP-Rab5-labeled early endosomes in the cells. In this case, cells were rinsed three times with phosphate-buffered saline (PBS) and fixed for 20 min with 4% paraformaldehyde (w/v in PBS) at room temperature. The coverslips were then directly processed for microscopy or used for further immunofluorescence microscopy to identify endogenous Rab5, Rabex-5, Rab22, and EEA1. In this case, the fixed cells were permeabilized with 0.1% saponin or Triton X-100 (w/v in PBS), and probed with the anti-Rab5, anti-Rabex-5, anti-Rab22, and anti-EEA1 antibodies from BD Bio-

sciences, Proteintech Group, and Santa Cruz Biotechnology (Santa Cruz, CA), respectively. The secondary antibodies were goat anti-mouse IgG conjugated to Alexa568 (red) and goat anti-rabbit IgG conjugated to Alexa488 (green) or Alexa647 (blue) (Invitrogen). The coverslips were then mounted in PBS on glass slides and viewed with a microscope.

Glutathione Transferase (GST) Pull-Down Assay

We cloned the cDNAs of Rab5 and Rab22 into the pGEX-4T-2 vector (GE Healthcare) and the resulting pGEX-4T-2/Rab5 and pGEX-4T-2/Rab22 constructs were then used to transform the *Escherichia coli* strain DH5 α and to express GST-Rab5 and GST-Rab22 fusion proteins, respectively. GST-Rab5 and GST-Rab22 were then affinity purified with glutathione-Sepharose 4B resin (GE Healthcare) and loaded with guanosine 5'-O-(3-thio)triphosphate (GTP γ S) or guanosine 5'-O-(2-thio)diphosphate (GDP β S) (Sigma-Aldrich) for the pull-down assays with various Rabex-5 proteins. Each Rabex-5 protein contained a Myc epitope at the N terminus and was expressed via the pBI vector in BHK cells for 24 h at 37°C. The cells were then washed with ice-cold PBS and lysed for 5 min in the lysis buffer, which contained 25 mM HEPES, pH 7.4, 100 mM NaCl, 5 mM MgCl₂, 0.1% NP-40, 10% glycerol, 1 mM dithiothreitol, and protease inhibitor cocktail (Sigma-Aldrich). Lysates were clarified by centrifugation at 10,000 \times g for 2 min at 4°C, and the supernatants (180 μ l) were incubated with 20 μ l (20 μ g) of the GST-Rab5 or GST-Rab22 fusion proteins on the glutathione-Sepharose 4B resin for 30 min at 4°C on a rotating mixer. The resin was subsequently rinsed with the lysis buffer, resuspended in SDS sample buffer, boiled for 3 min, and subjected to SDS-PAGE (12% gel), followed by immunoblot analysis with the anti-Myc antibody.

Epidermal Growth Factor (EGF) Endocytosis and Degradation

NF73 cells were grown on glass coverslips in 35-mm culture dishes and transfected with pEGFP-N1/EGFR and pBI constructs expressing various Myc-tagged Rabex-5 proteins, respectively, for 24 h. Then the growth medium was replaced with a HEPES-buffered medium containing Alexa555-EGF (5 ng/ml) (Invitrogen) and bovine serum albumin (2 mg/ml) and incubated for 10 min at 37°C. Cells were then washed four times with the HEPES-buffered medium without Alexa555-EGF and chased in the same medium for 0, 0.5, 2, and 4 h at 37°C. The cells were rinsed, fixed, and processed for confocal immunofluorescence microscopy as described above. In this case, the immunofluorescence staining was to confirm the expression of Myc-tagged Rabex-5 proteins with an anti-Myc mAb and a secondary goat anti-mouse IgG conjugated to Alexa647. The fluorescence of epidermal growth factor receptor (EGFR)-enhanced (e)GFP and Alexa555-EGF was directly observed in the same cells. The total fluorescence intensity of Alexa555-EGF in the cell was quantified with 60 randomly selected cells that also contained EGFR-eGFP and the indicated Myc-Rabex-5 construct in each experiment. The SEM was obtained from three independent experiments.

RESULTS

Rabex-5 Is a Rab22 Effector and Targets to Rab22-containing Early Endosomes

In the process of examining Rabex-5 interactions with Rab5 subfamily members in pull-down assays, we identified an interaction between Rabex-5 and Rab22, which surprisingly exhibited a binding profile distinct from that of Rabex-5 and Rab5 interaction. GST fusion proteins of Rab22 and Rab5 on glutathione Sepharose beads were loaded with GTP γ S or GDP β S and used to pull-down various Rabex-5 constructs expressed in BHK cells. The Rabex-5 constructs included the full-length protein (FL, residues 1-492), the GEF domain (residues 135-399), and the EET domain (residues 81-230), and each contained an N-terminal myc epitope for immunoblot detection (Figure 1A). Rab5 loaded with GDP β S but not GTP γ S was associated with the GEF domain (Figure 1B), in support of its high GEF activity toward Rab5 (Delprato *et al.*, 2004). Full-length Rabex-5 showed no detectable binding to Rab5 (Figure 1B), consistent with the fact that it has little GEF activity toward Rab5 *in vitro* due to a block by the coiled-coil domain immediately downstream of the GEF domain (Delprato and Lambright, 2007; Zhu *et al.*, 2007). In contrast, full-length Rabex-5 effectively associated with Rab22 and only with its GTP γ S-loaded form (Figure 1B). The binding of Rabex-5 to Rab22-GTP seemed much stronger than the binding of the GEF domain to Rab5-GDP, based on

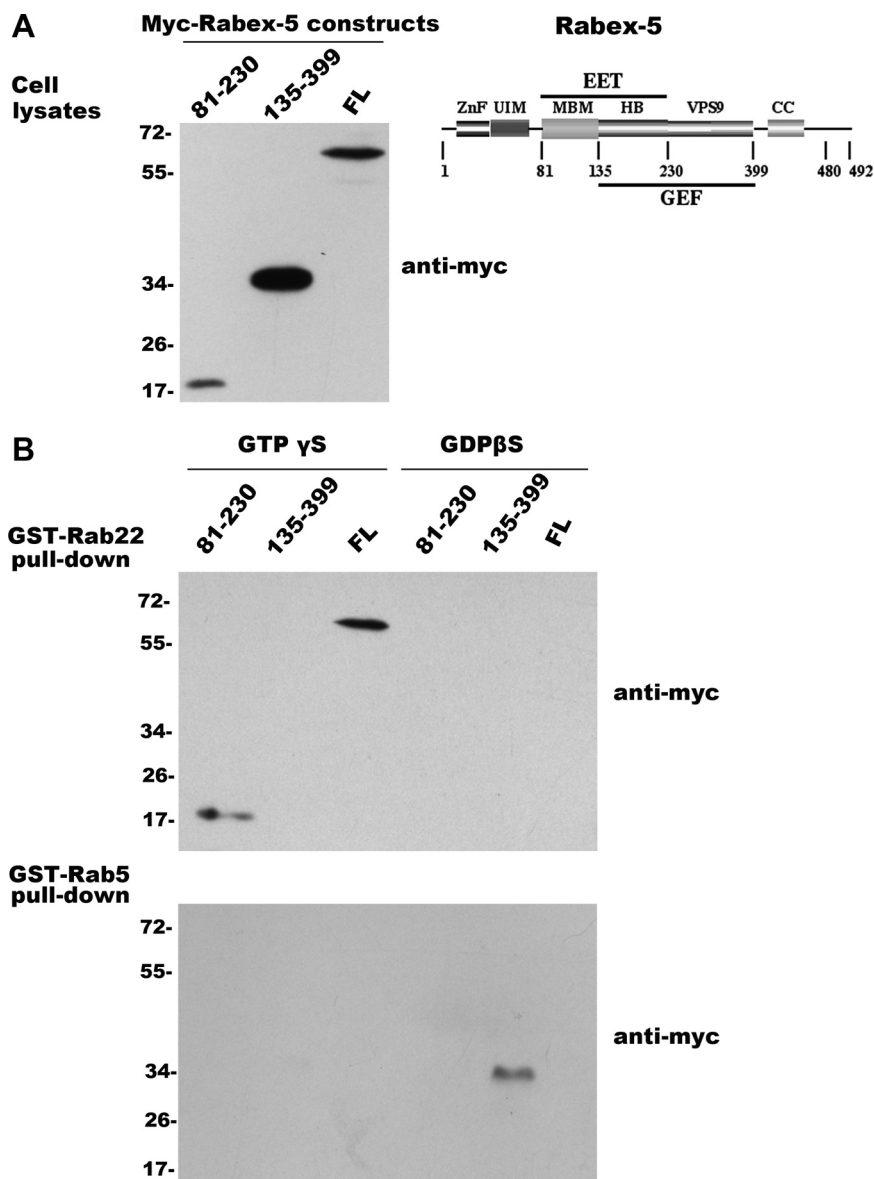


Figure 1. Rabex-5 differentially interacts with Rab22 and Rab5. (A) Schematic structure of Rabex-5 and immunoblot showing the input Myc-tagged Rabex-5 proteins expressed in BHK cells, including Myc-Rabex-5(81-230), Myc-Rabex-5(135-399), and Myc-Rabex-5(FL). The cells were transfected with the pBI constructs expressing the indicated Rabex-5 proteins and an aliquot (10 μ l) of each cell lysate (after clarification by centrifugation at 10,000 \times g) was subjected to immunoblot analysis with the anti-Myc antibody. The results were reproducible in two independent experiments. Molecular mass standards (in kilodaltons) are indicated on the left of the panel. The schematic structure illustrates the functional domains of Rabex-5 described in the text. (B) GST pull-down assays showing that Rab22 and Rab5 bind to different regions of Rabex-5, with distinct nucleotide requirement. GST-Rab22 and GST-Rab5 on glutathione-Sepharose 4B resin were loaded with either GTP γ S or GDP β S and then incubated with the cell lysates (180 μ l each, after clarification by centrifugation at 10,000 g) containing Myc-Rabex-5(81-230), Myc-Rabex-5(135-399), and Myc-Rabex-5(FL), respectively, as indicated. The bound Rabex-5 proteins on the resin were identified by immunoblot analysis with the anti-Myc antibody. The results were reproducible in two independent experiments. Molecular mass standards (in kilodaltons) are indicated on the left of the panels.

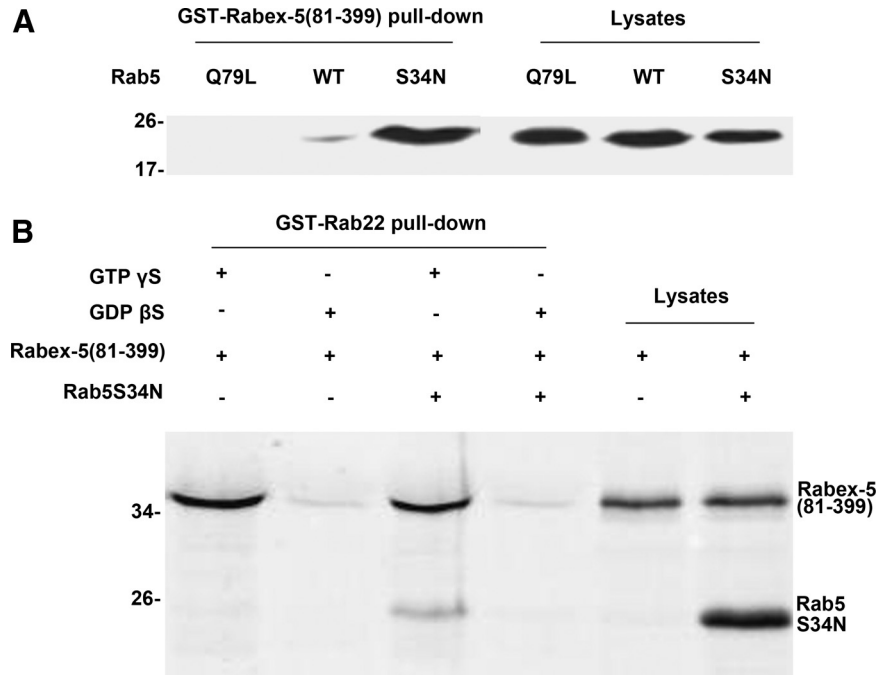
the ratio of pull-down signal over input (compare Figure 1A with Figure 1B). Importantly, the Rabex-5 and Rab22 interaction was mediated by the EET domain, which was bound to Rab22-GTP γ S, like the full-length protein (Figure 1B). Because the EET domain is essential for direct membrane targeting of Rabex-5 to early endosomes (Zhu *et al.*, 2007), the data suggest that Rab22 may recruit Rabex-5 to the early endosomes. We also included Rab21 and Rab31 in these pull-down assays. Rab21 interacted with Rabex-5 in the same manner as Rab5, whereas Rab31 was not associated with any of the Rabex-5 constructs tested (data not shown).

We confirmed the preference of Rabex-5 for GDP-bound Rab5 by using GST-Rabex-5(81-399) to pull-down various forms of Rab5: wild type (WT), Rab5:Q79L, and Rab5:S34N, expressed in BHK cells (Figure 2A). Rab5:Q79L and Rab5:S34N are two Rab5 mutants that are locked in GTP- and GDP-bound forms, due to defects in GTP hydrolysis and GTP binding, respectively. As expected, Rab5:S34N showed the most robust binding to GST-Rabex-5(81-399), followed by WT, whereas Rab5:Q79L showed no binding (Figure 2A). Next, we determined whether Rabex-5 can form a tripartite

complex with Rab22 and Rab5 by using GST-Rab22 to pull-down Rabex-5(81-399) and Rab5:S34N (Figure 2B). Rabex-5(81-399) was either expressed alone or coexpressed with Rab5:S34N in BHK cells and the cell lysates were used for pull-down assays by GST-Rab22 loaded with GTP γ S or GDP β S (Figure 2B). The results showed that GST-Rab22 efficiently pulled down Rabex-5(81-399) as well as associated Rab5:S34N in a GTP γ S-dependent manner (Figure 2B), suggesting formation of a tripartite complex of Rabex-5(81-399) and the two Rabs. The nucleotide-dependence of pull-down signals suggested specific protein interactions between Rab22 and Rabex-5(81-399)/Rab5:S34N rather than nonspecific binding to glutathione-Sepharose resin or GST.

Endogenous Rabex-5 and Rab22 colocalized in punctate endosomes in BHK cells, as determined by confocal immunofluorescence microscopy (Figure 3A). Although endogenous Rabex-5 signal on the membrane was relatively weak, the punctate staining pattern was consistently observed and was essentially identical to that of Rab22 (Figure 3A). Furthermore, coexpression of green fluorescent protein (GFP)-Rabex-5 and red fluorescent protein (RFP)-Rab22 in BHK

Figure 2. Tripartite complex of Rabex-5, Rab22 and Rab5. (A) GST-Rabex-5(81-399) pull-down of various forms of Rab5. Myc-Rab5:WT, Myc-Rab5:Q79L, and Myc-Rab5:S34N were expressed in BHK cells, respectively, and cell lysates were clarified by centrifugation at $10,000 \times g$. The postnuclear supernatants were either directly analyzed ($10 \mu\text{l}$) by immunoblot assays with the anti-Myc antibody to confirm protein expression or incubated ($180 \mu\text{l}$) with GST-Rabex-5(81-399) on glutathione-Sepharose 4B resin in the pull-down assays to determine protein interactions, as indicated. The results were reproducible in two independent experiments. Molecular mass standards (in kilodaltons) are indicated on the left of the panel. (B) GST-Rab22 pull-down of Rabex-5(81-399) and Rab5:S34N. Myc-Rabex-5(81-399) was either expressed alone or coexpressed with Myc-Rab5:S34N in BHK cells and cell lysates were clarified by centrifugation at $10,000 \times g$. The postnuclear supernatants were either directly analyzed ($10 \mu\text{l}$) by immunoblot assays with the anti-Myc antibody to confirm protein expression or incubated ($180 \mu\text{l}$) with GST-Rab22-GTP γ S or GST-Rab22-GDP β S on glutathione-Sepharose 4B resin in the pull-down assays to determine protein interactions, as indicated. The bound proteins on the resin were identified by immunoblot assays with the anti-Myc antibody. The results were reproducible in two independent experiments. Molecular mass standards (in kilodaltons) are indicated on the left of the panels.



cells showed complete colocalization of the two proteins in the early endosomes, which contained the early endosomal marker EEA1 and were significantly enlarged, as determined by confocal fluorescence microscopy (Figure 3B). The size increase of the early endosomes required the Rab5 GEF activity of Rabex-5, because GFP-Rabex-5(D314A), a mutant lacking the GEF activity (Delprato *et al.*, 2004), showed the same colocalization with RFP-Rab22, but these endosomes were much smaller and tended to cluster together (Figure 3). The clustered small endosomes were likely due to competition of the mutant with endogenous Rabex-5 for interaction with Rab22 and Rab5, leading to inhibition of endosome fusion. Moreover, GFP-Rabex-5(81-230), i.e., the EET domain, was sufficient for targeting to the RFP-Rab22-containing early endosomes in the cell (Figure 3), consistent with the pull-down data (Figure 1) and supporting our contention that Rab22 binds to the EET domain of Rabex-5 to recruit Rabex-5 to the membrane. In contrast, GFP-Rabex-5(135-399), i.e., the GEF domain, exhibited diffused cytosolic staining throughout the cell, and there was no colocalization with RFP-Rab22 and EEA1 on the early endosomes (Figure 3). Taken together, the data suggest that Rab22 may recruit Rabex-5 to the early endosomal membrane where Rabex-5 subsequently activates Rab5 to promote fusion and enlargement of these endosomes.

Inhibition of Rab22 via shRNA Blocks Membrane Targeting and Function of Rabex-5

Next, we investigated the effect of shRNA-mediated knockdown of Rab22 on the membrane targeting and function of Rabex-5. A previously described shRNA specific for human Rab22 (Magadan *et al.*, 2006) was used in this study and expressed in HeLa cells via the pSIREN-RetroQ-DsRed-Express vector, which simultaneously expressed dsRed-Express, an RFP, for identification of transfected cells by fluorescence microscopy. The effective knock down of Rab22

expression in the cell was confirmed by immunofluorescence microscopy with an anti-Rab22 antibody. Endogenous Rab22 showed punctate endosomal staining in the cytoplasm (Figure 4A), as reported previously (Weigert *et al.*, 2004; Magadan *et al.*, 2006). The Rab22 signal was dramatically reduced in transfected cells that expressed the Rab22-specific shRNA, which were identified by the red fluorescence in these cells (Figure 4A). As a negative control, expression of a scrambled shRNA had no effect on the Rab22 level in the cell (Figure 4A). Further immunoblot analysis of the cell lysates confirmed the effectiveness of the Rab22-specific shRNA, which reduced the Rab22 level by more than 80% in these cells (Figure 4B).

Coexpression of the Rab22-specific shRNA with GFP-Rabex-5 in HeLa cells revealed that the knockdown of Rab22 expression abrogated the direct targeting of GFP-Rabex-5 to early endosomes (Figure 4C). Cells that expressed only GFP-Rabex-5 showed that GFP-Rabex-5 efficiently targeted to EEA1-containing early endosomes and enlarged these endosomes as determined by confocal fluorescence microscopy (Figure 4C), consistent with the observation in BHK cells (Figure 4) (Zhu *et al.*, 2007). In contrast, cells that coexpressed the Rab22-specific shRNA with GFP-Rabex-5, as identified by the presence of both red and green fluorescence in the same cell, showed dramatic reduction in early endosome-associated GFP-Rabex-5, which instead was redistributed to the cytosol as evidenced by the diffuse green fluorescence throughout the cytoplasm (Figure 4C). Residual GFP-Rabex-5 could also be found on some small EEA1-containing endosomes (Figure 4C, arrows), which were not significantly enlarged, reflecting reduced recruitment of GFP-Rabex-5 on the membrane. In control cells that expressed a scrambled shRNA, GFP-Rabex-5 targeted normally to early endosomes and enlarged these endosomes (Figure 4C), like in the cells expressing GFP-Rabex-5 alone (Figure 4C).

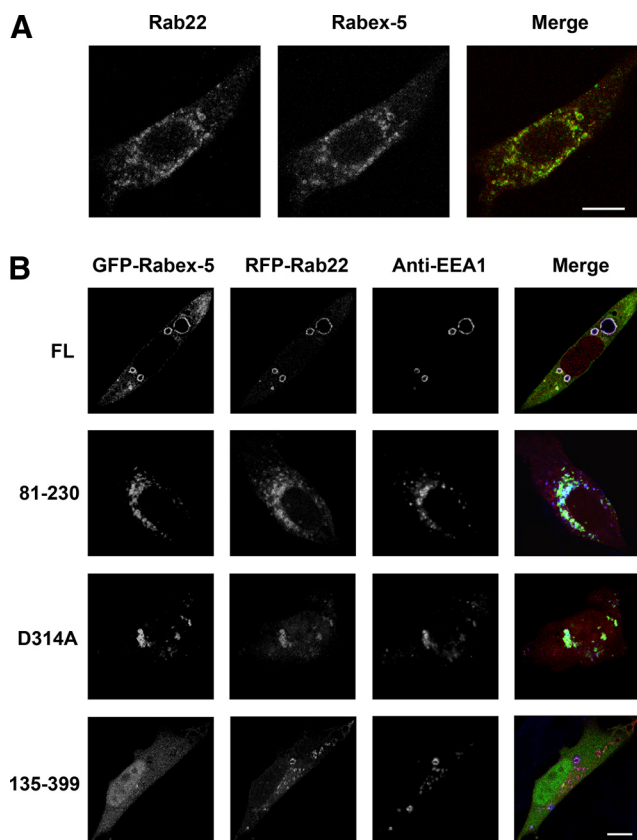


Figure 3. Rabex-5 targets to Rab22-containing early endosomes via the EET domain. (A) Confocal fluorescence microscopy showing colocalization of endogenous Rab22 and Rabex-5 in BHK cells. The cells were fixed, permeabilized, and immunostained with an anti-Rab22 rabbit polyclonal antibody and an anti-Rabex-5 mAb, followed by confocal fluorescence microscopy. The individual channels (green and red) are shown in black and white, whereas the merged image is shown in color. Bar, 8 μ m. (B) Confocal fluorescence microscopy showing colocalization of GFP-Rabex-5 with RFP-Rab22 on EEA1-containing early endosomes in BHK cells. Various GFP-tagged Rabex-5 constructs (green), as indicated, were coexpressed with RFP-Rab22 (red). The cells were fixed, permeabilized, and immunostained with an anti-EEA1 polyclonal antibody (blue), followed by confocal fluorescence microscopy. The individual channels (green, red, and blue) are shown in black and white, whereas the merged images are shown in color. Bar, 8 μ m.

The data showed that targeting of GFP-Rabex-5 to early endosomes was dependent on Rab22. Although Rabaptin-5 in Rab22-depleted cells could potentially bind to GFP-Rabex-5 and recruit it to the endosomes, endogenous Rabaptin-5 is limiting and already associated with endogenous Rabex-5 and thus unavailable to form new complexes with GFP-Rabex-5 (Zhu *et al.*, 2007). In support of this contention, coexpression of Rabaptin-5 with GFP-Rabex-5 was able to rescue the defective membrane targeting of GFP-Rabex-5 in Rab22-depleted cells (Supplemental Figure S1).

Rabex-5 Mediates Functional Synergy of Rab22 and Rab5 in Regulation of Early Endosomal Dynamics

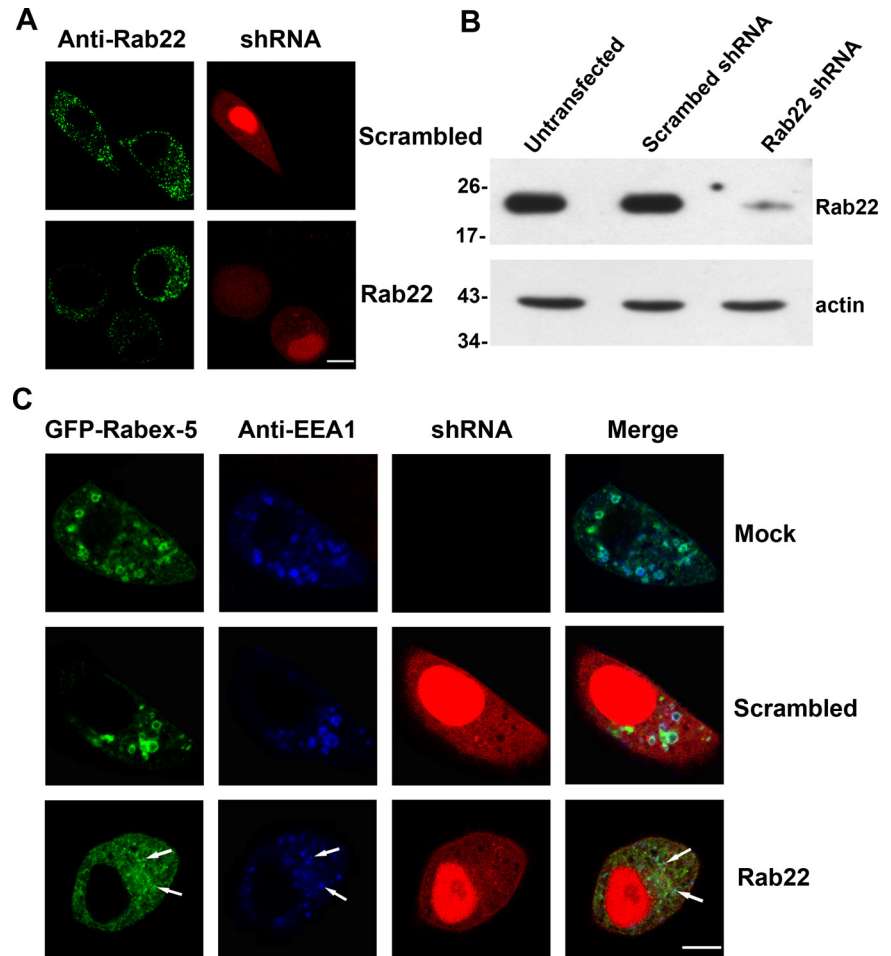
To determine how Rab22-mediated recruitment of Rabex-5 may impact Rab5 activation and early endosomal dynamics, we first examined, via confocal immunofluorescence microscopy, if endogenous Rab22 and Rab5 colocalize on early endosomes in BHK and NF73 cells. The latter was a Rabex-

5-deficient mouse embryo fibroblast line isolated from Rabex-5 knockout mice (Kalesnikoff *et al.*, 2007). In both cell types, Rab22 and Rab5 colocalized to punctate early endosomes (Figure 5A, arrows). However, the Rab5 staining on early endosomes in NF73 cells was consistently weaker, especially considering its much higher expression level in NF73 cells than in BHK cells (Figure 5B). NF73 cells might up-regulate Rab5 expression to compensate for the loss of Rabex-5. Alternatively, Rabex-5 as a ubiquitin ligase (Matera *et al.*, 2006) could target Rab5 for degradation, leading to lower steady-state level of Rab5 in normal cells. Another interesting observation was that the Rab22- and Rab5-containing early endosomes clustered at the perinuclear region in BHK cells, whereas they were evenly distributed throughout the cytoplasm in NF73 cells (Figure 5A). Both BHK and NF73 are fibroblasts with elongated morphology, in contrast to HeLa cells. The redistribution of early endosomes in NF73 cells seems to be due to Rabex-5 deficiency and reduced Rab5 activity, because expression of Rabex-5 in NF73 cells restored the perinuclear localization pattern of Rab5 and Rab22 (Figure 5A). The data are consistent with a role of Rab5 in regulation of early endosomal movement along the cytoskeleton (Nielsen *et al.*, 1999).

We next determined the effects of overexpression of Rab22 and Rab5 on early endosomal dynamics in BHK and NF73 cells. RFP-Rab22 and GFP-Rab5 were either expressed separately or coexpressed in the cells, followed by confocal fluorescence microscopy. In BHK cells, either RFP-Rab22 or GFP-Rab5 alone targeted to early endosomes, and enlarged these endosomes to some extent (Figure 5C) in comparison to their endogenous counterparts (Figure 5A). Coexpression of RFP-Rab22 and GFP-Rab5 showed colocalization of the two Rabs in the same early endosomes (Figure 5C). A striking observation was that the RFP-Rab22- and GFP-Rab5-containing early endosomes were much larger than those containing either RFP-Rab22 or GFP-Rab5 alone (Figure 5, C and D), suggesting a collaborative relationship of Rab22 and Rab5 in regulation of early endosome fusion. Importantly, the functional synergy of the two Rabs was dependent on Rabex-5, as evidenced by the uncoupling of Rab22 and Rab5 functions in NF73 cells. When expressed separately, RFP-Rab22-containing early endosomes showed dramatically distinct morphology from those containing GFP-Rab5 (Figure 5C). The former were dramatically enlarged, whereas the latter exhibited small punctate structures similar to endogenous early endosomes (Figure 5, C and D), suggesting enhanced Rab22-mediated endosome fusion but little change in Rab5 activity. Furthermore, coexpression of RFP-Rab22 and GFP-Rab5 showed only partial colocalization in NF73 cells, in contrast to the complete colocalization of the two Rabs in BHK cells (Figure 5C). RFP-Rab22-containing endosomes exhibited extreme heterogeneity in size, ranging from small to very large with GFP-Rab5 concentrated in the small ones (Figure 5C). The large RFP-Rab22-containing endosomes lacked GFP-Rab5 (Figure 5C, arrows). Along this line, the size of these large RFP-Rab22-containing endosomes was no different with or without coexpression of GFP-Rab5 in NF73 cells (Figure 5, C and D), in contrast to the functional synergy of the two Rabs in BHK cells (Figure 5, C and D). Rab22, like Rab5, can use EEA1 as an effector to promote early endosome fusion (Kauppi *et al.*, 2002). Our data can be reconciled if Rabex-5 competes with EEA1 for binding to Rab22-GTP on the early endosomes in normal cells, suppressing Rab22-mediated endosome fusion while activating Rab5-mediated endosome fusion.

Introduction of Rabex-5 into NF73 cells completely restored the colocalization of GFP-Rab5 and RFP-Rab22 on

Figure 4. Blocking Rab22 expression via shRNA abrogates direct membrane targeting and function of Rabex-5. (A) Confocal fluorescence microscopy showing knockdown of endogenous Rab22 by Rab22-specific shRNA in HeLa cells. Cells were transfected with pSIREN-RetroQ-DsRed-Express constructs expressing either a Rab22-specific or a scrambled shRNA as indicated. Transfected cells were identified by dsRed expression whose red fluorescence is distributed throughout cytoplasm and in nucleus. Rab22 in transfected cells (with red fluorescence) as well as untransfected cells (without red fluorescence) was identified by immunofluorescence microscopy with the anti-Rab22 antibody (green). The results were reproducible in two independent experiments. Bar, 8 μ m. (B) Immunoblot confirming the knockdown of endogenous Rab22 by Rab22-specific shRNA in HeLa cells. Cell lysates from either untransfected cells as a control or transfected cells expressing scrambled or Rab22-specific shRNA were subjected to immunoblot analysis with the anti-Rab22 antibody. The same membrane was also probed with the anti-actin antibody, as a loading control. Molecular mass standards (in kilodaltons) are indicated on the left side of the panels. The results were reproducible in three independent experiments. (C) Confocal fluorescence microscopy showing that shRNA-mediated Rab22 knockdown blocks membrane targeting of Rabex-5 to early endosomes in HeLa cells. Cells were either mock transfected as a control or transfected with the pSIREN-RetroQ-DsRed-Express constructs expressing Rab22-specific or scrambled shRNAs as indicated (red). GFP-Rabex-5 (green) was coexpressed in these cells via pBI vector. At 48 h posttransfection, the cells were fixed, permeabilized, and immunostained with the anti-EEA1 polyclonal antibody (blue), followed by confocal fluorescence microscopy. The results were reproducible in three independent experiments. Bar, 8 μ m.



enlarged early endosomes (Figure 5C). Like Rabex-5, Rabex-5(1-399) and Rabex-5(135-480) were also able to restore the colocalization of GFP-Rab5 and RFP-Rab22 on enlarged endosomes in NF73 cells (Supplemental Figure S2). Rabex-5(135-480) lacks the Rab22-binding domain, but it can target to early endosomes indirectly via association with Rabaptin-5 in NF73 cells. Expression of Rabex-5:D314A, a mutant without Rab5 GEF activity, inhibited early endosome fusion and resulted in colocalization of GFP-Rab5 and RFP-Rab22 in clustered small endosomes (Supplemental Figure S2). The data suggest that Rab5 and Rab22 target to the same early endosomes and Rabex-5 plays a key role in maintaining their colocalization in the cell. In the absence of Rabex-5, increased Rab22-mediated membrane fusion, without accompanied increase in Rab5-mediated fusion, may contribute to the separation of the two Rabs into different populations of endosomes.

The function of the Rab22-Rabex-5-Rab5 cascade was further examined by determining endocytosis and degradation of EGF in the Rabex-5-deficient NF73 cells. The uptake of Alexa555-EGF was monitored by confocal fluorescence microscopy. To facilitate EGF endocytosis, NF73 cells were transfected with a construct expressing EGFR-GFP and the transfected cells showed strong uptake of Alexa555-EGF that colocalized with EGFR-GFP in punctate endosomes (data not shown). To determine the kinetics of Alexa555-EGF deg-

radation, an initial 10-min uptake was followed by different times of chase in fresh medium without Alexa555-EGF. It was apparent that the degradation kinetics was very slow in these cells (Figure 6). Immediately after the uptake, Alexa555-EGF showed up in punctate endosomes in all cells containing EGFR-GFP. The total fluorescence intensity of Alexa555-EGF in the cell gradually decreased over time due to degradation in late endosomes/lysosomes (Figure 6). However, there were still 50% of Alexa555-EGF retained in the cell after a 4-h chase (Figure 6). In comparison, coexpression of Rabex-5 in these cells greatly accelerated Alexa555-EGF degradation, with nearly 80 and 90% degradation achieved within 2 and 4 h, respectively (Figure 6). At these times, the Alexa555-EGF fluorescence signal was dramatically reduced and was beyond detection in most cells. The Rabex-5-facilitated EGF degradation was mediated by its activation of Rab5, because the Rabex-5:D314A mutant lacking Rab5 GEF activity failed to increase Alexa555-EGF degradation (Figure 6).

Rabex-5 can activate Rab5 via the newly identified Rab22-Rabex-5-Rab5 cascade or indirectly via association with Rabaptin-5 that binds to Rab5-GTP in a positive feedback loop (Lippe *et al.*, 2001). To distinguish the two Rabex-5 pathways, we took advantage of the two Rabex-5 constructs: Rabex-5(1-399) and Rabex-5(135-480) that can use the direct and indirect pathways, respectively (Zhu *et al.*, 2007). Rabex-

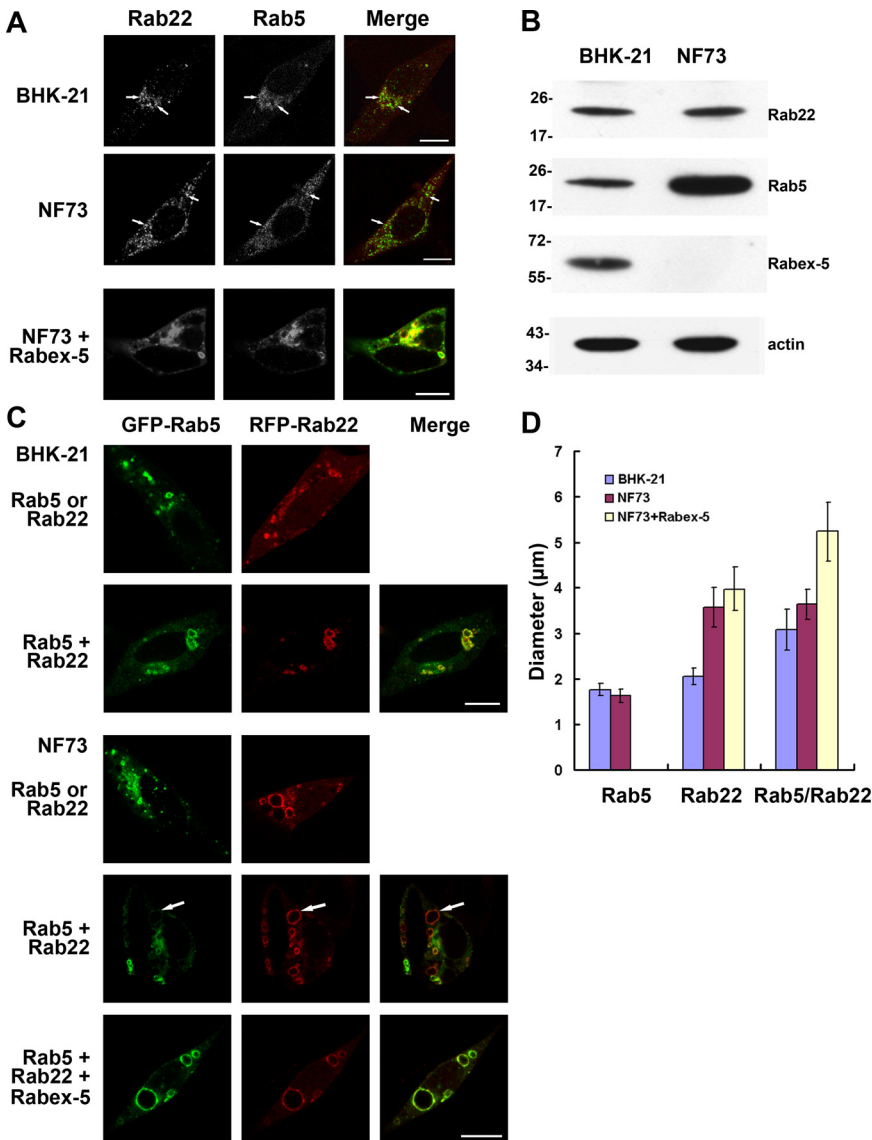


Figure 5. Functional synergy of Rab22 and Rab5 on early endosomes requires Rabex-5. **A.** Confocal fluorescence microscopy showing colocalization of endogenous Rab22 and Rab5 in BHK and NF73 cells. NF73 cells were either observed directly or after expression of Rabex-5 as indicated. The cells were fixed, permeabilized, and immunostained with an anti-Rab22 rabbit polyclonal antibody and an anti-Rab5 mAb, followed by confocal fluorescence microscopy. The individual channels (green and red) are shown in black and white, whereas the merged images are shown in color. Bar, 8 μ m. **(B)** Immunoblot showing endogenous levels of Rab5, Rab22, and Rabex-5 in BHK and NF73 cells. Cell lysates were subjected to SDS-PAGE, followed by immunoblot analysis with the anti-Rab5, anti-Rab22, and anti-Rabex-5 antibodies as indicated. The same membrane was also probed with the anti-actin antibody, as a loading control. Molecular mass standards (in kilodaltons) are indicated on the left side of the panels. The results were reproducible in two independent experiments. **(C)** Confocal fluorescence microscopy showing synergistic enlargement of early endosomes by GFP-Rab5 and RFP-Rab22 in BHK cells but not in Rabex-5-deficient NF73 cells. GFP-Rab5 and RFP-Rab22 were expressed either separately or together in the cells, as indicated, followed by confocal fluorescence microscopy. The coexpression of Myc-Rabex-5 in the bottom panel was confirmed by immunofluorescence microscopy (data not shown). The results were reproducible in three independent experiments. Bar, 8 μ m. **D.** Quantification of early endosomal size in BHK and NF73 cells. The graph shows the maximal size of early endosomes labeled by GFP-Rab5 alone, RFP-Rab22 alone, or both of the Rabs. In each case, the diameters of 100 of the largest endosomes in \sim 40 cells were measured and shown are the mean and calculated SEM.

5(1-399) contains the EET domain for binding to Rab22 and targets to early endosomes directly, but lacks the Rabaptin-5-binding domain. In contrast, Rabex-5(135-480) contains the Rabaptin-5-binding domain, but lacks the EET domain. Expression of Rabex-5(1-399), like Rabex-5, strongly increased Alexa555-EGF degradation in the cell (Figure 6). Rabex-5(135-492) was also able to increase Alexa555-EGF degradation, but the kinetics was much slower (Figure 6). The data suggest that the Rab22-Rabex-5-Rab5 cascade is functionally important in promoting a faster and efficient endocytic pathway for ligand/receptor degradation, e.g., EGF and EGFR.

DISCUSSION

Membrane targeting to early endosomes is critical for Rabex-5 to activate Rab5 that is associated with early endosomes in the cell. A well-documented membrane targeting mechanism is mediated by Rabaptin-5, a Rab5 effector that binds to Rab5-GTP (Stenmark *et al.*, 1995; Zhu *et al.*, 2004). In this case, Rabex-5 forms a complex with Rabaptin-5 and the complex targets to early endosomes via Rabaptin-5 binding

to Rab5-GTP on the membrane (Lippe *et al.*, 2001). Here, we identify a novel membrane targeting pathway that directly recruits Rabex-5 to early endosomes via binding to Rab22-GTP on the early endosomes.

Our finding that Rabex-5 differentially interacts with Rab5 and Rab22 is consistent with previous observations that Rabex-5 shows strong GEF activity toward Rab5 but not Rab22 (Delprato *et al.*, 2004). Indeed, our pull-down results indicate that Rabex-5 interacts with GDP-bound but not GTP-bound Rab5. In contrast, Rabex-5 binds to GTP-bound Rab22, establishing Rabex-5 as a Rab22 effector. Rabex-5 binds Rab22 via its EET domain (residues 81-230), which is immediately upstream of the catalytic Vps9 domain (residues 231-400). Interestingly, Rabex-5 binds to Rabaptin-5 via a coiled-coil domain (residues 401-462) immediately downstream of the Vps9 domain (Mattera *et al.*, 2006; Delprato and Lambright, 2007; Kalesnikoff *et al.*, 2007; Zhu *et al.*, 2007). Thus, Rabex-5 targets to the early endosomes directly or indirectly via two domains flanking the catalytic Vps9 domain that acts on Rab5-GDP and stimulates its GDP dissociation and GTP loading.

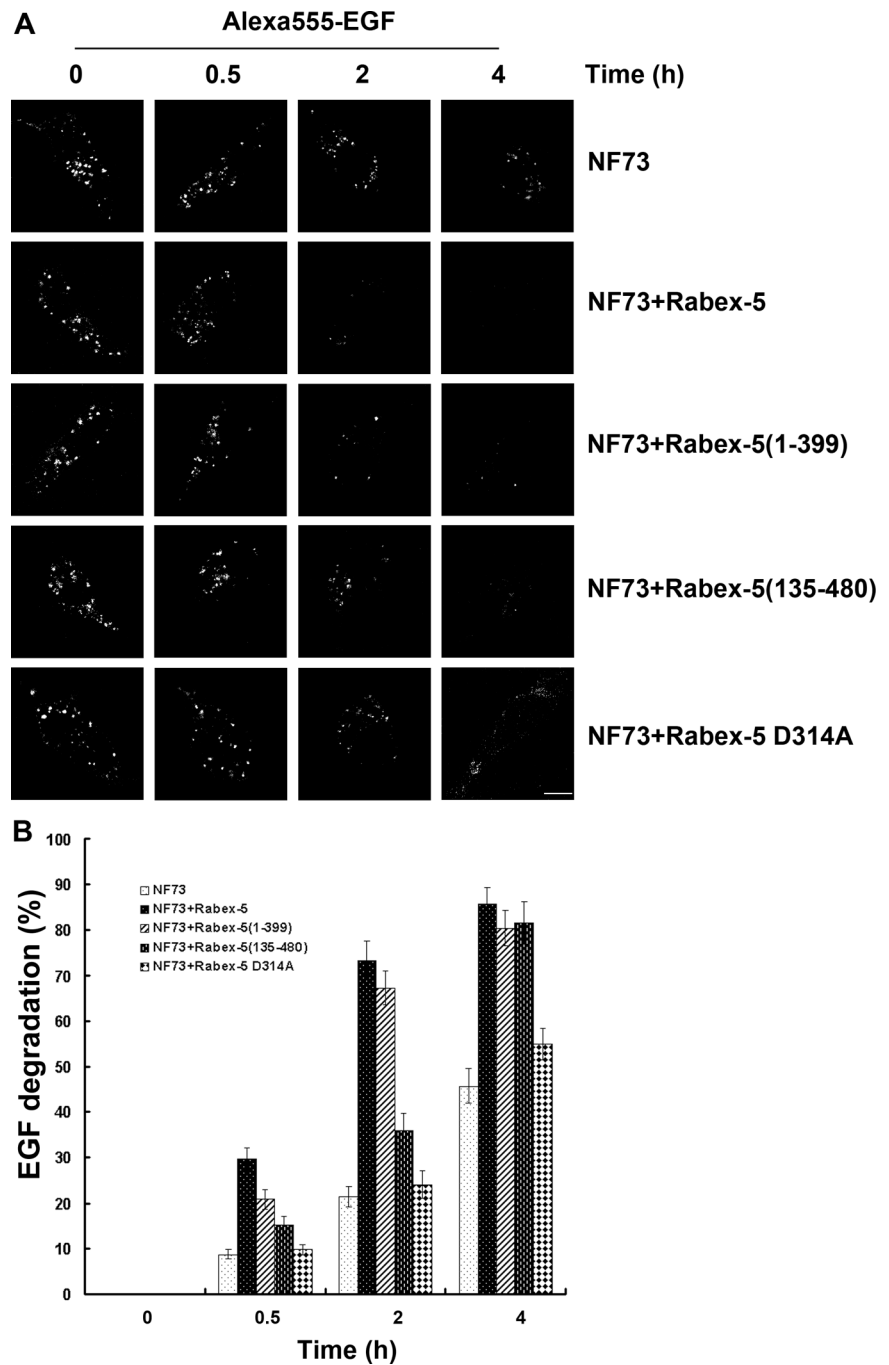


Figure 6. Rab22–Rabex-5–Rab5 cascade promotes degradation of endocytosed EGF. (A) Confocal fluorescence microscopy showing clearance of internalized Alexa555-EGF over time in NF73 cells without or with the indicated Rabex-5 proteins. Alexa555-EGF (5 ng/ml) was internalized for 10 min, followed by 0-, 0.5-, 2-, and 4-h chase as indicated. Representative images show the amount of Alexa555-EGF remaining in the cell at each time point in control NF73 cells or cells expressing Myc-Rabex-5, Myc-Rabex-5(1-399), Myc-Rabex-5(135-480), or Myc-Rabex-5:D314A. Similar expression levels of the Myc-tagged Rabex-5 proteins in these cells were confirmed by immunostaining with an anti-Myc mAb and goat anti-mouse IgG conjugated to Alexa647 (data not shown). Bar, 8 μ m. (B) Quantification of Alexa555-EGF degradation described in A. In each case, 60 cells were measured for the fluorescence intensity of Alexa555-EGF in the cell. The fluorescence intensity at 0 min is standardized as 100%. The graph shows percent of fluorescence loss (degradation) over time. Error bars represent SEM from three independent experiments.

Rab22-GTP recruits Rabex-5 to the membrane, which in turn acts on Rab5-GDP to convert it to Rab5-GTP. This Rab22-Rab5 signaling pathway represents a new Rab GTPase cascade in the regulation of early endosomal dynamics. In mammalian cells, the Rab5 subfamily of Rab GTPases contains four highly related members including Rab5, Rab21, Rab22, and Rab31 (also called Rab22b) (Pereira-Leal and Seabra, 2000; Stenmark and Olkkonen, 2001). Three of them, Rab5, Rab21, and Rab22, reside in the early endosomes. Like Rab5, Rab21 seems to promote early endosome fusion and receptor-mediated endocytosis (Simpson *et al.*, 2004). Importantly, Rab21 is as a good substrate as Rab5 for the GEF activity of Rabex-5 (Delprato *et al.*, 2004). Thus, the Rab22-Rab5 cascade should include Rab21 and the recruit-

ment of Rabex-5 by Rab22-GTP may lead to activation of both Rab5 and Rab21, suggesting a temporal convergence of functional Rab domains on the early endosomal membrane. Our data show that Rabex-5 is necessary for functional coupling of Rab22 and Rab5 in early endosome fusion. Endogenous Rab22 and Rab5 activities are limited, as evidenced by punctate small early endosomal structures in normal cells, and coexpression of Rab22 and Rab5 leads to synergistic enlargement of the early endosomes. However, this functional synergy is lost in Rabex-5-deficient NF73 cells. In this case, expression of Rab22 alone dramatically enlarges the endosomes, whereas expression of Rab5 has little effect. Thus, although Rabex-5 activates Rab5 as a GEF, it inhibits Rab22 as an effector at the same time in endosome

fusion, presumably by competing with EEA1 for binding to Rab22-GTP on the endosomal membrane. Our data suggest that Rab22- and Rab5-mediated endosome fusions are functionally distinct in early endosomal sorting and Rabex-5 level in the cell determines which type of fusion and sorting prevails. The Rab22–Rabex-5–Rab5 cascade promotes Rab5-mediated endosome fusion, which in turn promotes endocytic traffic and degradation of encytosed ligands, e.g., EGF.

The identification of Rab22–Rabex-5–Rab5 signaling cascade supports a general concept of Rab cascade in regulation of intracellular membrane trafficking. The first Rab-GEF–Rab cascade was identified in the yeast exocytic pathway where two homologous Rabs Ypt31 and Ypt32p, in the GTP-bound form, recruit Sec2p to the Golgi membrane (Ortiz *et al.*, 2002). Sec2p is a GEF for the downstream Rab Sec4p that promotes transport of Golgi-derived vesicles to the plasma membrane (Walch-Solimena *et al.*, 1997); thus, Sec2p activates Sec4p and functionally links Ypt31p/32p and Sec4p to promote exocytosis (Ortiz *et al.*, 2002). A variation on the theme is the TRANsport Protein Particle complex that switches its GEF specificity from Ypt1 to Ypt31 via incorporation of additional subunits (Morozova *et al.*, 2006). In mammalian systems, the Rab5–Rab7 conversion that occurs during the transition from early endosomes to late endosomes is suggested to involve a Rab cascade mediated by two components of the class C VPS/HOPS complex, Vps11p and Vps39p (Rink *et al.*, 2005). Vps11p is a Rab5 effector, whereas Vps39p contains GEF activity for Ypt7 (Wurmser *et al.*, 2000) and is assumed to contain GEF activity for its mammalian homolog Rab7. This assumption, however, remains to be established. Our current study identifies a Rab22–Rabex-5–Rab5 signaling cascade within the early endosomal network and suggests another layer of complexity in the regulation of early endosomal dynamics.

The Rab22-mediated recruitment of Rabex-5 to early endosomes is distinct from the ubiquitin-mediated Rabex-5 recruitment reported recently (Mattera and Bonifacino, 2008), because the EET domain, in the absence of N-terminal ZnF and MIU domains, is necessary and sufficient for binding to Rab22-GTP and targeting to Rab22-containing early endosomes. The relationship of the two membrane targeting pathways is unclear at present, but they are not mutually exclusive and both may contribute to the association of Rabex-5 with early endosomes. Direct targeting of Rabex-5 to early endosomes activates Rab5, which in turn recruits Rabaptin-5/Rabex-5 complexes that further activates Rab5 and produces more Rab5-GTP to maintain the Rab5 domain (Horiuchi *et al.*, 1997; Lippe *et al.*, 2001). With the identification of Rabex-5 as a Rab22 effector, a new Rab GTPase cascade emerges within the early endosomal network that begins with Rab22-mediated activation of Rab5 and/or Rab21, which is then followed by linkage to Rab7 for further trafficking along the endocytic pathway (Rink *et al.*, 2005).

ACKNOWLEDGMENTS

We thank Gillian Air for critical reading of the manuscript, Stephen Galli and Eon Rios (Stanford University) for kindly providing the NF73 cells, Alexander Sorkin (University of Colorado) for kindly providing the plasmid peGFP-N1/EGFR Brian Ceresa for advice on EGF degradation assays, and Jim Henthorn for expert assistance in confocal fluorescence microscopy. This work was supported in part by National Institutes of Health grant R01 GM-074692 (to G. L.).

REFERENCES

Bucci, C., Parton, R. G., Mather, I. M., Stunnenberg, H., Simons, K., Hoflack, B., and Zerial, M. (1992). The small GTPase Rab5 functions as a regulatory factor in the early endocytic pathway. *Cell* 70, 715–728.

Christoforidis, S., McBride, H. M., Burgoyne, R. D., and Zerial, M. (1999). The Rab5 effector EEA1 is a core component of endosome docking. *Nature* 397, 621–625.

Delprato, A., and Lambright, D. G. (2007). Structural basis for Rab GTPase activation by VPS9 domain exchange factors. *Nat. Struct. Mol. Biol.* 14, 406–412.

Delprato, A., Merithew, E., and Lambright, D. G. (2004). Structure, exchange determinants, and family-wide rab specificity of the tandem helical bundle and Vps9 domains of Rabex-5. *Cell* 118, 607–617.

Grosshans, B. L., Ortiz, D., and Novick, P. (2006). Rabs and their effectors: achieving specificity in membrane traffic. *Proc. Natl. Acad. Sci. USA* 103, 11821–11827.

Horiuchi, H., *et al.* (1997). A novel Rab5 GDP/GTP exchange factor complexed to Rabaptin-5 links nucleotide exchange to effector recruitment and function. *Cell* 90, 1149–1159.

Kalesnikoff, J., Rios, E. J., Chen, C. C., Alejandro Barbieri, M., Tsai, M., Tam, S. Y., and Galli, S. J. (2007). Roles of RabGEF1/Rabex-5 domains in regulating Fc epsilon RI surface expression and Fc epsilon RI-dependent responses in mast cells. *Blood* 109, 5308–5317.

Kauppi, M., Simonsen, A., Bremnes, B., Vieira, A., Callaghan, J., Stenmark, H., and Olkkonen, V. M. (2002). The small GTPase Rab22 interacts with EEA1 and controls endosomal membrane trafficking. *J. Cell Sci.* 115, 899–911.

Lanzetti, L., Palamidessi, A., Areces, L., Scita, G., and Di Fiore, P. P. (2004). Rab5 is a signalling GTPase involved in actin remodelling by receptor tyrosine kinases. *Nature* 429, 309–314.

Li, G., Barbieri, M. A., Colombo, M. I., and Stahl, P. D. (1994). Structural features of the GTP-binding defective Rab5 mutants required for their inhibitory activity on endocytosis. *J. Biol. Chem.* 269, 14631–14635.

Lippe, R., Miaczynska, M., Rybin, V., Runge, A., and Zerial, M. (2001). Functional synergy between Rab5 effector Rabaptin-5 and exchange factor Rabex-5 when physically associated in a complex. *Mol. Biol. Cell* 12, 2219–2228.

Magadan, J. G., Barbieri, M. A., Mesa, R., Stahl, P. D., and Mayorga, L. S. (2006). Rab22a regulates the sorting of transferrin to recycling endosomes. *Mol. Cell Biol.* 26, 2595–2614.

Mattera, R., and Bonifacino, J. S. (2008). Ubiquitin binding and conjugation regulate the recruitment of Rabex-5 to early endosomes. *EMBO J.* 27, 2484–2494.

Mattera, R., Tsai, Y. C., Weissman, A. M., and Bonifacino, J. S. (2006). The Rab5 guanine nucleotide exchange factor Rabex-5 binds ubiquitin (Ub) and functions as a Ub ligase through an atypical Ub-interacting motif and a zinc finger domain. *J. Biol. Chem.* 281, 6874–6883.

Morozova, N., Liang, Y., Tokarev, A. A., Chen, S. H., Cox, R., Andrejic, J., Lipatova, Z., Sciorra, V. A., Emr, S. D., and Segev, N. (2006). TRAPP II subunits are required for the specificity switch of a Ypt-Rab GEF. *Nat. Cell Biol.* 8, 1263–1269.

Nielsen, E., Severin, F., Backer, J. M., Hyman, A. A., and Zerial, M. (1999). Rab5 regulates motility of early endosomes on microtubules. *Nat. Cell Biol.* 1, 376–382.

Olkkonen, V. M., Dupree, P., Killisch, I., Lutcke, A., Zerial, M., and Simons, K. (1993). Molecular cloning and subcellular localization of three GTP-binding proteins of the rab subfamily. *J. Cell Sci.* 106, 1249–1261.

Ortiz, D., Medkova, M., Walch-Solimena, C., and Novick, P. (2002). Ypt32 recruits the Sec4p guanine nucleotide exchange factor, Sec2p, to secretory vesicles; evidence for a Rab cascade in yeast. *J. Cell Biol.* 157, 1005–1015.

Pereira-Leal, J. B., and Seabra, M. C. (2000). The mammalian Rab family of small GTPases: definition of family and subfamily sequence motifs suggests a mechanism for functional specificity in the Ras superfamily. *J. Mol. Biol.* 301, 1077–1087.

Rink, J., Ghigo, E., Kalaidzidis, Y., and Zerial, M. (2005). Rab conversion as a mechanism of progression from early to late endosomes. *Cell* 122, 735–749.

Simonsen, A., Lippe, R., Christoforidis, S., Gaullier, J. M., Brech, A., Callaghan, J., Toh, B. H., Murphy, C., Zerial, M., and Stenmark, H. (1998). EEA1 links PI(3)K function to Rab5 regulation of endosome fusion. *Nature* 394, 494–498.

Simpson, J. C., Griffiths, G., Wessling-Resnick, M., Fransen, J. A., Bennett, H., and Jones, A. T. (2004). A role for the small GTPase Rab21 in the early endocytic pathway. *J. Cell Sci.* 117, 6297–6311.

Stenmark, H., and Olkkonen, V. M. (2001). The Rab GTPase family. *Genome Biol.* 2, REVIEWS3007.

- Stenmark, H., Parton, R. G., Steele-Mortimer, O., Lutcke, A., Gruenberg, J., and Zerial, M. (1994). Inhibition of rab5 GTPase activity stimulates membrane fusion in endocytosis. *EMBO J.* *13*, 1287–1296.
- Stenmark, H., Vitale, G., Ullrich, O., and Zerial, M. (1995). Rabaptin-5 is a direct effector of the small GTPase Rab5 in endocytic membrane fusion. *Cell* *83*, 423–432.
- Walch-Solimena, C., Collins, R. N., and Novick, P. J. (1997). Sec2p mediates nucleotide exchange on Sec4p and is involved in polarized delivery of post-Golgi vesicles. *J. Cell Biol.* *137*, 1495–1509.
- Weigert, R., Yeung, A. C., Li, J., and Donaldson, J. G. (2004). Rab22a regulates the recycling of membrane proteins internalized independently of clathrin. *Mol. Biol. Cell* *15*, 3758–3770.
- Wurmser, A. E., Sato, T. K., and Emr, S. D. (2000). New component of the vacuolar class C-Vps complex couples nucleotide exchange on the Ypt7 GTPase to SNARE-dependent docking and fusion. *J. Cell Biol.* *151*, 551–562.
- Zerial, M., and McBride, H. (2001). Rab proteins as membrane organizers. *Nat. Rev. Mol. Cell Biol.* *2*, 107–117.
- Zhu, G., Zhai, P., Liu, J., Terzyan, S., Li, G., and Zhang, X. C. (2004). Structural basis of Rab5-Rabaptin5 interaction in endocytosis. *Nat. Struct. Mol. Biol.* *11*, 975–983.
- Zhu, H., Zhu, G., Liu, J., Liang, Z., Zhang, X. C., and Li, G. (2007). Rabaptin-5-independent membrane targeting and Rab5 activation by Rabex-5 in the Cell. *Mol. Biol. Cell* *18*, 4119–4128.